Vol 13 No 1, January 2004
1009-1963/2004/13(01)/0040-07

Chinese Physics

© 2004 Chin. Phys. Soc.
and IOP Publishing Ltd

A unified incompressible lattice BGK model and its application to three-dimensional lid-driven cavity flow*

He Nan-Zhong(何南忠)[a], Wang Neng-Chao(王能超)[a)b)],
Shi Bao-Chang(施保昌)[b)c)†], and Guo Zhao-Li(郭照立)[c)]

[a)] *School of Computer Science and Technology, Huazhong University of Science and Technology, Wuhan* 430074, *China*
[b)] *Department of Mathematics, Huazhong University of Science and Technology, Wuhan* 430074, *China*
[c)] *State Key Laboratory of Coal Combustion, Huazhong University of Science and Technology, Wuhan* 430074, *China*

(Received 21 March 2003; revised manuscript received 4 June 2003)

A unified lattice Bhatnagar–Gross–Krook (ILBGK) model iD*d*Q*q* for the incompressible Navier–Stokes equation is presented. To test its efficiency, the lid-driven cavity flow in three-dimensional space for Reynolds number Re=3200 and span aspect ratio SAR=1, 2 and 3 is simulated in detail on a $48 \times 48 \times (48 \times \mathrm{SAR})$ uniform lattice using the model. The test results agree well with those in previous experiments and numerical works and show the efficiency and strong numerical stability of the proposed ILBGK model.

Keywords: unified incompressible lattice BGK model, incompressible Navier–Stokes equation, three-dimensional lid-driven cavity flow
PACC: 4700, 0270, 0520D

1. Introduction

The lattice Boltzmann method (LBM) is a relatively new approach that uses simple microscopic kinetic models to simulate complicated macroscopic behaviour of transport phenomena. Compared with the conventional computational fluid dynamics (CFD) approach based on discretizations of macroscopic continuum equations, the LBM is simple in form, of high performance computationally, and intrinsically parallel. It is also easy to incorporate complicated boundary conditions such as those in porous media. In recent years, the LBM method has achieved great success in simulations of fluid flows and modelling physics in fluids, involving complicated boundaries or/and complex fluids, such as turbulent flow, the Rayleigh–Taylor instability between two fluids, multi-phase/component fluids, free boundaries in flow systems, particle suspensions in fluid, reactive–diffusive systems and combustions, pattern formation, magnetohydrodynamics, crystal growing, granular flow and others.[1−15]

The LB models commonly used in the solution of incompressible Navier–Stokes equations can be viewed as compressible schemes to simulate incompressible fluid flows, and there is the compressible effect which might lead to some undesirable errors in numerical simulations. Some LB models have been proposed to reduce or eliminate such errors.[4−6] However, most of the existing LB models either can be used only to simulate steady flows or are still of artificial compressible form. So, when used to simulate unsteady incompressible flows, these methods require some additional conditions to neglect the artificial compressible effect. In Ref.[7], we proposed a 9-bit incompressible LBGK (ILBGK) model, the incompressible D2Q9 LBGK, in two-dimensional space. To our knowledge, this model is the first one without compressible effect for simulating incompressible flows. The model can be used in the solution of steady or unsteady problems and has strong numerical stability.[7−10]

Although the potential of the LBM as a viable CFD tool has been demonstrated in simulations of complex fluids, its application to flows at high

*Project supported by the National Natural Science Foundation of China (Grant Nos 60073044 and 70271069), and the State Key Development Program for Basic Research of China (Grant No G1999022207).
†Corresponding author. E-mail: sbchust@yahoo.com

Reynolds number (Re) or/and in three-dimensional space remains as an area of future development. Recently we have successfully used our ILBGK model and its thermal version with a robust boundary scheme [10] to simulate some typical flows at high Re in two-dimensional space.[8−10] In this paper, we present a unified ILBGK model iDdQq based on the common DdQq lattice [11] using the idea in Ref.[7]. To test the efficiency of the model, the benchmarking problem, lid-driven cavity flow, in three-dimensional space for Re=3200 and span aspect ratio SAR=1, 2 and 3 on $48\times48\times(48\times\text{SAR})$ uniform lattice is simulated in detail using the model. The test results agree well with those in previous works [14−18] and show the efficiency and numerical stability of the ILBGK model proposed in the paper.

2. Incompressible DdQq LBGK model iDdQq

A popular LB model is the so-called lattice BGK model (LBGK) with the single relaxation time approximation [1]

$$\begin{aligned} &g_i(\boldsymbol{x}+c\boldsymbol{e}_i\Delta t, t+\Delta t)-g_i(\boldsymbol{x},t)\\ =&-\tau^{-1}[g_i(\boldsymbol{x},t)-g_i^{(\mathrm{eq})}(\boldsymbol{x},t)], \end{aligned} \tag{1}$$

where $\boldsymbol{e}_i$ is the discrete velocity direction, and $c=\Delta x/\Delta t$ is the particle speed, Δx, Δt, and τ are the lattice grid spacing, the time step and the dimensionless relaxation time, respectively. $g_i(\boldsymbol{x},t)$ is the distribution function at node $\boldsymbol{x}$ and time t with velocity $\boldsymbol{e}_i$, and $g_i^{(\mathrm{eq})}(\boldsymbol{x},t)$ is the corresponding equilibrium distribution depending on the lattice model used.

The commonly used lattice model is the DdQq model given by Qian,[11] where d is the dimension and q is the number of the discrete velocity directions. Unlike the common LBGK models, we take the pressure p as an independent variable in the equilibrium distribution as in Ref.[7] to derive a unified ILBGK model, iDdQq. The equilibrium distribution in iDdQq is defined as

$$g_i^{(\mathrm{eq})}=\lambda_i p+s_i(\boldsymbol{u}), \tag{2}$$

where λ_i is the parameter to be defined below, $s_i(\boldsymbol{u})=\omega_i\left[\dfrac{(c\boldsymbol{e}_i\cdot\boldsymbol{u})}{c_s^2}+\dfrac{(c\boldsymbol{e}_i\cdot\boldsymbol{u})^2}{2c_s^4}-\dfrac{|\boldsymbol{u}|^2}{2c_s^2}\right]$, ω_i are the weight coefficients such that $\omega_i>0$, $\sum\limits_{i\geq0}\omega_i=1$, and c_s is the sound speed. They also depend on the lattice model.[11]

For the iD2Q9 model,[7] we have ω_0=4/9, ω_i=1/9 (i=1:4), and ω_i=1/36 (i=5:8), $c_s=c/\sqrt{3}$, while $\lambda_0=-5/(3c^2)$, $\lambda_i=1/(3c^2)$ (i=1:4) and $\lambda_i=1/(12c^2)$ (i=5:8).

For the general iDdQq model, λ_i in $g_i^{(\mathrm{eq})}$ can be determined by the following constraints:

$$\sum_{i\geq0}g_i^{(\mathrm{eq})}=0,\quad \sum_{i\geq0}c\boldsymbol{e}_i g_i^{(\mathrm{eq})}=\boldsymbol{u},$$

$$\sum_{i\geq0}c^2\boldsymbol{e}_i\boldsymbol{e}_i g_i^{(\mathrm{eq})}=p\boldsymbol{I}+\boldsymbol{u}\boldsymbol{u}. \tag{3}$$

As in Ref.[7], we take $\lambda_i=\alpha\omega_i$ for $i>0$, then from the first and last constraints above we have

$$\lambda_0=-\sum_{i>0}\lambda_i,\quad \alpha\sum_{i>0}c^2\omega_i\boldsymbol{e}_i\boldsymbol{e}_i p=\alpha c_s^2 p\boldsymbol{I}=p\boldsymbol{I}, \tag{4}$$

leading to

$$\lambda_i=\omega_i/c_s^2,\quad \lambda_0=-\sum_{i>0}\omega_i/c_s^2=(\omega_0-1)/c_s^2. \tag{5}$$

The flow velocity, pressure and kinetic viscosity are given by

$$\boldsymbol{u}=\sum_{i\geq0}c\boldsymbol{e}_i g_i,$$

$$p=-\lambda_0^{-1}\left[\sum_{i>0}g_i+s_0(\boldsymbol{u})\right]=\frac{c_s^2}{1-\omega_0}\left[\sum_{i>0}g_i+s_0(\boldsymbol{u})\right],$$

$$\nu=(\tau-1/2)c_s^2\Delta t. \tag{6}$$

For the iD3Q15 model, $c_s=c/\sqrt{3}$, ω_0=2/9, ω_i=1/9 ($i=1-6$), ω_i=1/72 ($i=7-14$), and for the iD3Q19 one, $c_s=c/\sqrt{3}$, ω_0=1/3, ω_i=1/18 ($i=1-6$), ω_i=1/36 ($i=7-18$).[3,11]

Now the iDdQq model is well defined. Through multi-scaling expansion, the true incompressible Navier–Stokes equation can be derived to the second order under the low Mach number limitation:[7]

$$\nabla\cdot\boldsymbol{u}=0, \tag{7}$$

$$\frac{\partial\boldsymbol{u}}{\partial t}+\boldsymbol{u}\cdot\nabla\boldsymbol{u}=-\nabla p+\nu\nabla^2\boldsymbol{u}. \tag{8}$$

3. Numerical results

To test the efficiency of the model, the benchmarking problem (lid-driven cavity flow) in three dimensions for different Re and span aspect ratios (SAR) is simulated in detail using the model. The configuration of the driven cavity flow considered consists of a three-dimensional cavity whose top wall moves from left to right with a uniform velocity, while the nonslip boundary condition is employed on the other

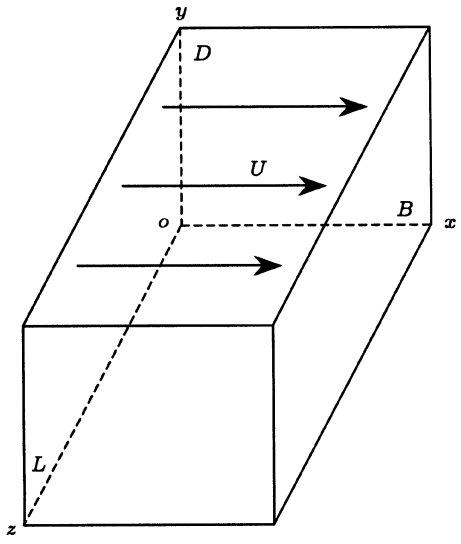


Fig.1. Configuration of the driven cavity flow.

five walls (see Fig.1). The flow is assumed to be Newtonian fluid described by the incompressible Navier–Stokes equations (7) and (8). The Reynolds number is $Re = BU/\nu$, where B is the width of the cavity, U is the uniform velocity of the moving wall. In the simulations, we take U=1, $B = D = 1$, and the span-to width ratio (SAR=$L : B$) is set to 1, 2 and 3.

Numerical simulations were carried out using the model presented above for the driven cavity flow with Re=1,000–6,000 on a 48 × 48 × (48×SAR) uniform lattice for SAR=1, 2 and 3, respectively. The iD3Q19 model was used for all cases. We found that the iD3Q15 model could only simulate the flow at $Re \leq 2,000$ on the lattice here, and it blew up when simulating the flow at $Re > 2,000$, say Re=3,200. So the iD3Q19 model has a stronger numerical stability than the iD3Q15 one. In the simulations, the relaxation parameter $\omega = 1/\tau$ is taken from 1.92 to 1.986, Δt determined by Eq.(6) with $c_s^2 = c^2/3 = \Delta x^2/(3\Delta t^2)$ is about 0.003, and the particle speed $c = \Delta x/\Delta t$ is set in the range 6.0–8.0. The initial condition is set at p=0, and the velocities at all nodes, except the top nodes, are set at $u = v = w = 0$. The boundary conditions were treated by the nonequilibrium extrapolation scheme.[10] All simulations were performed on a P4 (1.4G) personal computer, and the computational cost of 5,600 iterations of the iD3Q19 model for SAR 1:1 case required about one hour of CPU time.

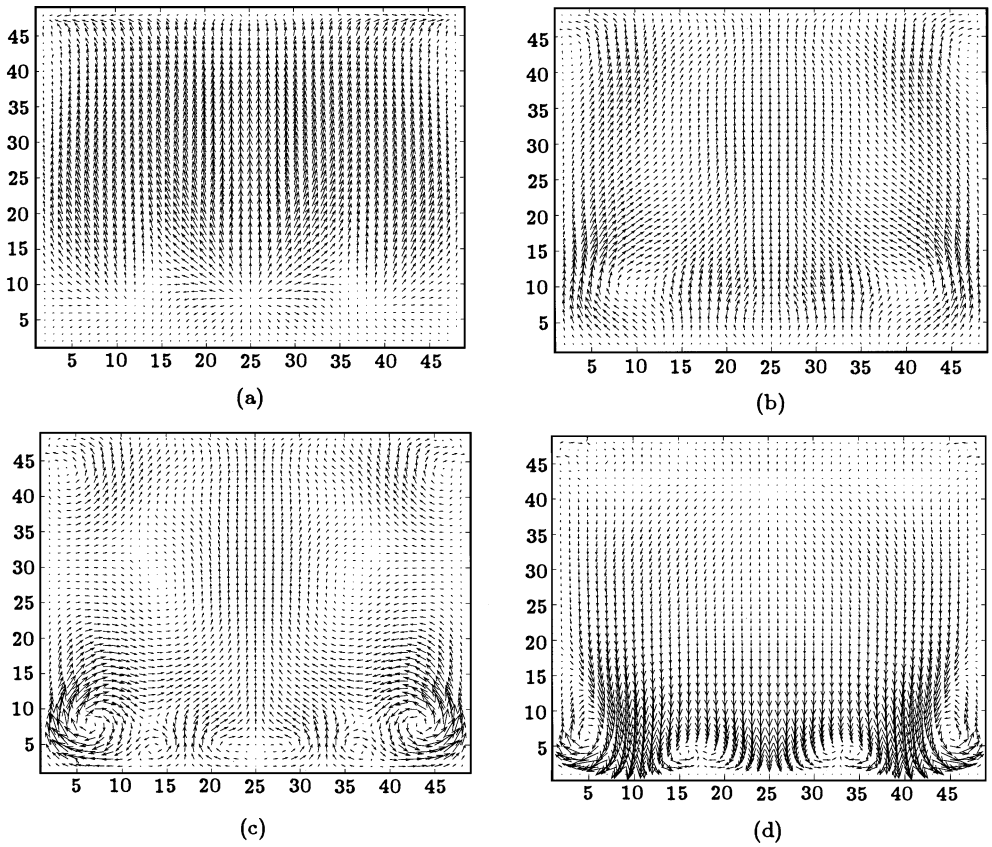


Fig.2. Velocity vector plots in the yz-plane of a cubic cavity for Re=3,200 at 50,000 time steps. (a) x=0.0625; (b) x=0.375; (c) x=0.5; (d) x=0.75.

In this paper we only give the simulation results for the flow at Re=3,200 since more experimental and numerical results have been obtained for this case. The parameters $\omega = \tau^{-1}$, Δt and c are taken as 1.974, 0.003049 and 6.8331, respectively. The velocity vector plots in the yz- and xz-planes of the cubic cavity for Re=3,200 at 50,000 time step are shown in Figs.2 and 3. Figures 4 and 5 show the velocity vector plots in the yz-planes of the cavity of SAR=2 and 3 for Re=3,200 at different time steps. From Figs.2 and 3 we can see that the flow structures in the specified planes agree well with those in Refs.[14–16], and two pairs of Taylor–Görtler like (TGL) vortices are clearly visible along the span. It can be found from Figs.4 and 5 that the number of TGL vortices varies from four to six for SAR 2:1 cavity and from seven to nine for the SAR 3:1 case, and the location and number of these vortices vary with time. The results here for SAR 3:1 case agree with those reported in experiments and numerical simulations.[15] As for the SAR 2:1 case we have not found the report about the number of TGL vortices in the literature, and we predict that seven pairs of TGL vortices may be found if a finer lattice is used in simulation. It is noteworthy that the ratio of lattice sizes used here and in LBM based models in Refs.[14,15] in each direction is 48:128, and the lattice size used here is close to those in simulations of the same problem by conventional CFD methods.[16–18] This greatly enhances the computational ability of the LBM. In fact, we can use an even coarser lattice than that used here, but the accuracy may be lower. Figure 6 illustrates some results obtained in simulation on a $40 \times 40 \times (40 \times \mathrm{SAR})$ lattice. If the nonuniform LB technique is used, the accuracy is expected to be improved. To know the global behaviour of the cavity flow, three-dimensional streamlines of the flow for Re=3,200 and SAR=1, 2 are plotted in Fig.7.

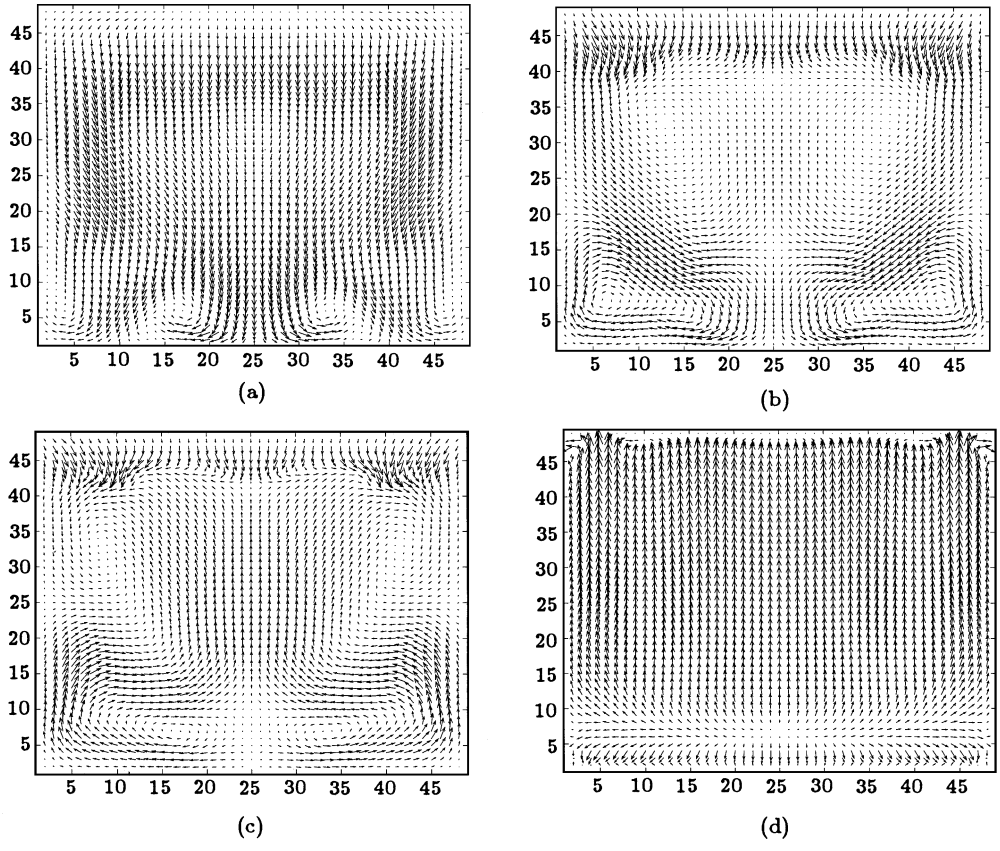


Fig.3. Velocity vector plots in the xz-plane of a cubic cavity for Re=3,200 at 50,000 time steps. (a) y=0.25; (b) y=0.5; (c) y=0.625; (d) y=0.9375.

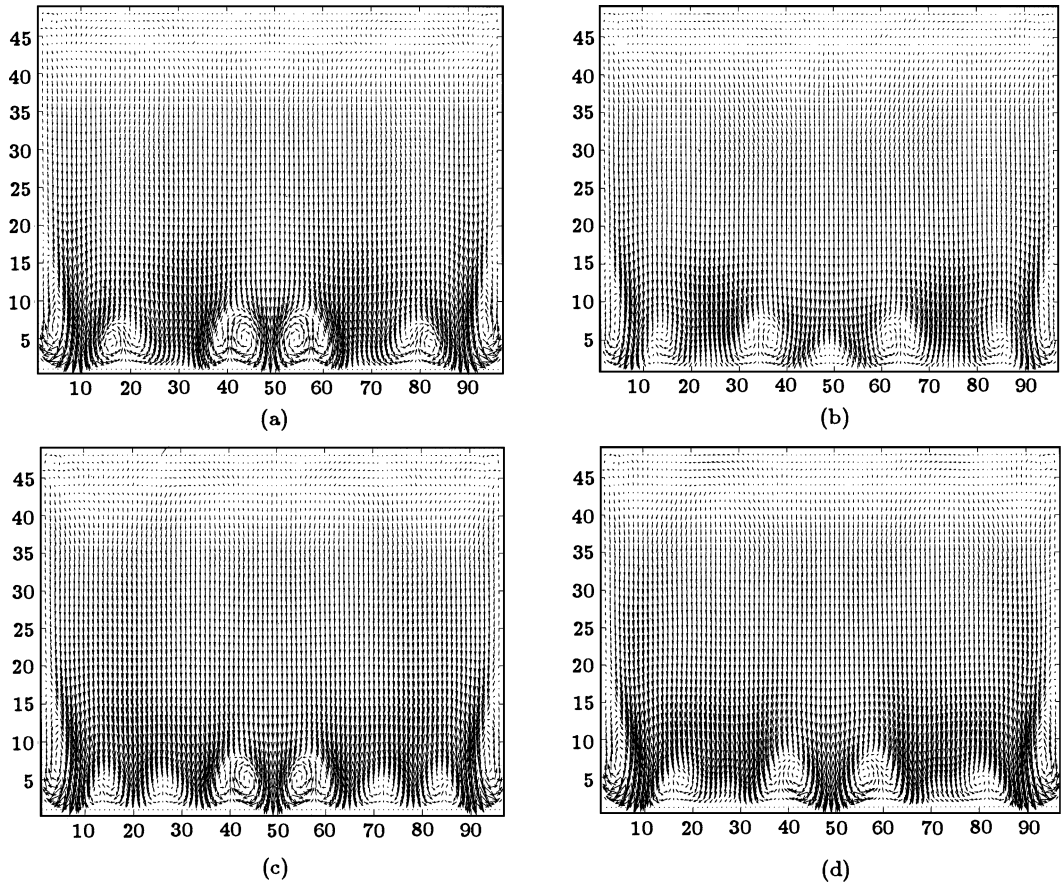


Fig.4. Velocity vector plots in the yz-plane of a rectangular cavity of aspect ratio 1:1:2 for Re=3,200 at x=0.75. (a) to (d): t=36,000, 48,000, 58,000 and 74,000.

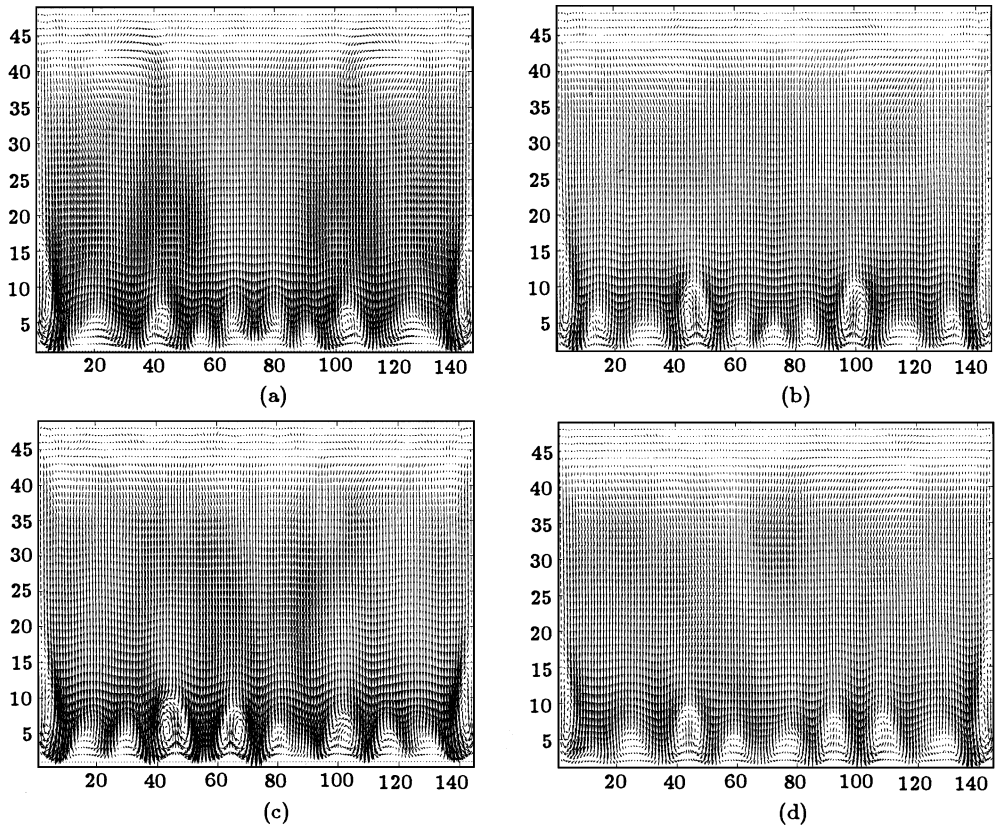


Fig.5. Velocity vector plots in the yz-plane of a rectangular cavity of aspect ratio 1:1:3 for Re=3,200 at x=0.75. (a) to (d): t=22,000, 34,000, 62,000 and 78,000.

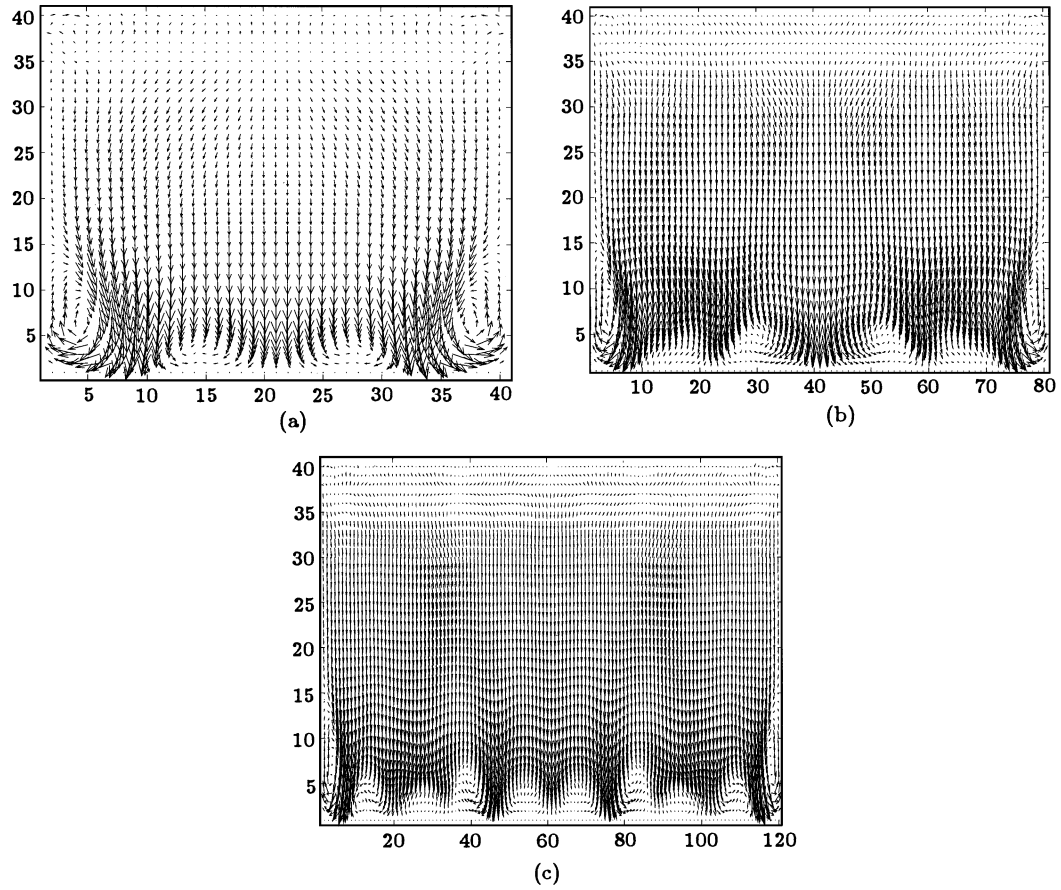


Fig.6. Velocity vector plots in the yz-plane of the cavity for Re=3,200 and SAR=1, 2 and 3 at x=0.75. (a) to (c): t=48,000, 42,000, and 40,000.

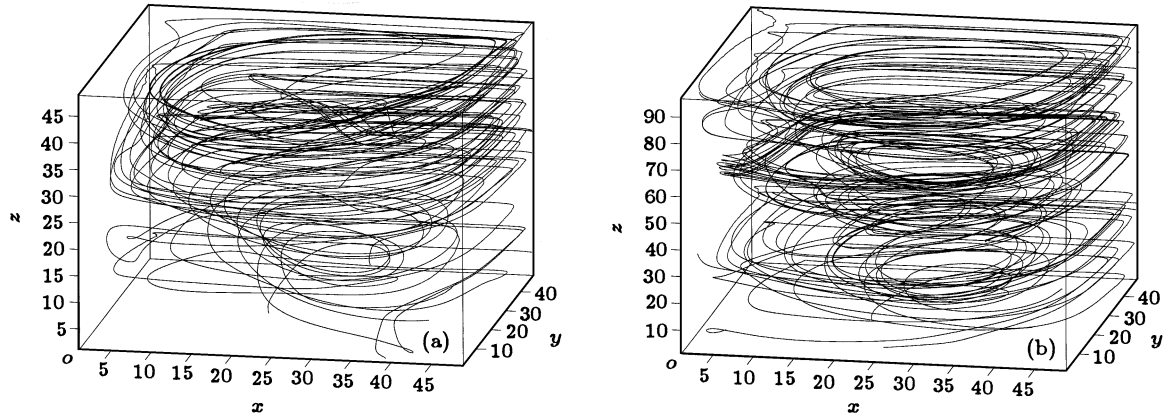


Fig.7. Three-dimensional streamlines of the cavity for Re=3,200 and SAR=1, 2. (a) to (b): t=50,000 and 58,000.

4. Conclusion

We have presented a unified LBGK model for the incompressible Navier–Stokes equation. Utilizing a robust boundary processing scheme, the nonequilibrium extrapolation rule,[10] the incompressible flow at larger Re can be simulated accurately on coarser uniform lattice by using the model, which is verified by the numerical tests for three-dimensional lid-driven cavity flow for different Re and SAR. We have found that other LBGK models with this scheme also have better stability. It is well known that the numerical stability of the LBGK models is usually very poor as $\omega = \tau^{-1} \to 2$ ($\omega \in (0,2)$ from Eq.(6)). We found

that our scheme is still stable and accurate even for ω=1.986, at which the computation blows up using other schemes for the boundary conditions. In fact, selecting $\omega \in (0, 2)$, $c(\gg |\boldsymbol{u}|)$, etc., properly in their stable regions (here $\omega \in (0, 1.986]$, $c \approx 7$) according to Eq.(6), we can simulate the flows at different Re, large or small. Our results indeed show the advantages of the LBM.

References

[1] Chen S Y and Doolen G D 1998 *Annu. Rev. Fluid Mech.* **30** 32

[2] Luo L S 2000 *Proc. Int. Conf. Appl. CFD* (Beijing) p52

[3] Guo Z L, Zheng C G, Li Q and Wang N C 2002 *Lattice Boltzmann Method for Hydrodynamics* (Wuhan: Hubei Science & Technology Press) (in Chinese)

[4] He X and Luo L S 1997 *J. State Phys.* **88** 927

[5] Lin Z, Fang H and Tao R 1997 *Phys. Rev.* E **54** 6323

[6] Zou Q, Hou S, Chen S and Doolen G 1995 *J. State Phys.* **81** 35

[7] Guo Z L, Shi B C and Wang N C 2000 *J. Comput. Phys.* **165** 288

[8] Shi B C, Guo Z L and Wang N C 2002 *Chin. Phys. Lett.* **19** 515

[9] Guo W B, Wang N C, Shi B C and Guo Z L 2003 *Chin. Phys.* **12** 67

[10] Guo Z L, Zheng C G and Shi B C 2002 *Chin. Phys.* **11** 366

[11] Qian Y, d'Humieres D and Lallemand P 1992 *Europhys. Lett.* **17** 479

[12] Liu M R *et al* 1999 *Acta Phys. Sin.* **48** 1800 (in Chinese)

[13] Lu X Y and Li H B 2001 *Acta Phys. Sin.* **50** 422 (in Chinese)

[14] Hou S 1995 *PhD Thesis* Kansas State University, Manhattan

[15] Teixeira C M 1997 *Int. J. Mod. Phys.* C **8** 685

[16] Kato Y, Kawai H and Tanahashi T 1999 *JSME Int. J.* Ser. II **33** 649

[17] Chiang T P, Sheu W H and Hwang R R 1998 *Int. J. Numer. Meth. Fluids* **26** 557

[18] Migeon C 2002 *Exp. Fluids* **33** 594